climate

MDPI

Article

Snow Resources and Climatic Variability in Jammu and Kashmir, India

Aaqib Ashraf Bhat [1], Poul Durga Dhondiram [1], Saurabh Kumar Gupta [1,*], Shruti Kanga [2], Suraj Kumar Singh [1], Gowhar Meraj [3], Pankaj Kumar [4] and Bhartendu Sajan [1]

[1] Centre for Climate Change & Water Research (C3WR), Suresh Gyan Vihar University, Jaipur 302017, India; ashrafaaqib498@gmail.com (A.A.B.); poul.2246456@mygyanvihar.com (P.D.D.); suraj.kumar@mygyanvihar.com (S.K.S.); bhartendu.sajan@mygyanvihar.com (B.S.)
[2] Department of Geography, School of Environment and Earth Sciences, Central University of Punjab, VPO-Ghudda, Bathinda 151401, India; shruti.kanga@cup.edu.in
[3] Graduate School of Agricultural and Life Sciences, The University of Tokyo, 1-1-1 Yayoi, Tokyo 113-8654, Japan
[4] Institute for Global Environmental Strategies, Hayama 240-0115, Japan; kumar@iges.or.jp
* Correspondence: saurabhkr.gupta@mygyanvihar.com

Abstract: Climate change is profoundly impacting snow-dependent regions, altering hydrological cycles and threatening water security. This study examines the relationships between snow water equivalent (SWE), snow cover, temperature, and wind speed in Jammu and Kashmir, India, over five decades (1974–2024). Using ERA5 reanalysis and Indian Meteorological Department (IMD) datasets, we reveal significant declines in SWE and snow cover, particularly in high-altitude regions such as Kupwara and Bandipora. A Sen's slope of 0.0016 °C per year for temperature highlights a steady warming trend that accelerates snowmelt, shortens snow cover duration, and reduces streamflow during critical agricultural periods. Strong negative correlations between SWE and temperature ($r = -0.7$ to -0.9) emphasize the dominant role of rising temperatures in SWE decline. Wind speed trends exhibit weaker correlations with SWE ($r = -0.2$ to -0.4), although localized effects on snow redistribution and evaporation are evident. Temporal snow cover analyses reveal declining winter peaks and diminished summer runoff contributions, exacerbating water scarcity. These findings highlight the cascading impacts of climate variability on snow hydrology, water availability, and regional ecosystems. Adaptive strategies, including real-time snow monitoring, sustainable water management, and climate-resilient agricultural practices, are imperative for mitigating these challenges in this sensitive Himalayan region.

Keywords: snow water equivalent; IMD; ERA 5; hailstorm; climate; agriculture; water resources; natural disaster

Academic Editor: Christina Anagnostopoulou

Received: 13 November 2024
Revised: 23 January 2025
Accepted: 25 January 2025
Published: 30 January 2025

Citation: Bhat, A.A.; Dhondiram, P.D.; Gupta, S.K.; Kanga, S.; Singh, S.K.; Meraj, G.; Kumar, P.; Sajan, B. Snow Resources and Climatic Variability in Jammu and Kashmir, India. *Climate* **2025**, *13*, 28. https://doi.org/10.3390/cli13020028

1. Introduction

Snow resources are vital components of global hydrological systems [1], acting as natural reservoirs that regulate water availability for ecosystems [2], agriculture [3], and human use [4]. However, rising temperatures and altered precipitation patterns, driven by climate change, threaten these resources [5]. Declining snowmelt volumes and altered timing of snowmelt exacerbate water scarcity during critical agricultural periods, jeopardizing food security and increasing the frequency of extreme events such as floods,

droughts, and wildfires [6]. Addressing these challenges requires a detailed understanding of snow resource variability and its cascading impacts on socio-environmental systems. The dynamics of snow resources are influenced by various climatic and geographical factors, including temperature, precipitation, wind speed, and topography [7]. Rising temperatures accelerate snowmelt, reducing snow cover duration, while wind speeds alter snow deposition and sublimation rates [8]. These changes are compounded by regional climate variability, which can intensify extreme weather events such as floods, droughts, wildfires, and hailstorms [9]. Addressing these challenges requires a comprehensive understanding of snow resource dynamics and their cascading impacts on socio-environmental systems. A key metric for quantifying snow resources is the Snow Water Equivalent (SWE), which represents the water content stored in snowpacks [10]. SWE provides critical insights into the hydrological balance and the seasonal availability of water [11]. Despite its importance, localized studies on SWE trends and their drivers remain scarce, particularly in complex terrains such as the Himalayas [12]. This knowledge gap highlights the need for region-specific analyses to better understand the interactions between climatic variables and snow resources.

Jammu and Kashmir, a region located in the western Himalayas, represents the challenges posed by declining snow resources. This region relies heavily on snowmelt for water supply, agriculture, and hydropower generation [13]. Rising temperatures in the area—reported at an annual increase of 0.04 to 0.05 °C—have accelerated snowmelt and shortened snow cover duration, even as winter precipitation remains relatively stable [14]. Kolahoi Glacier, a critical water source for the Jhelum River, has lost 23% of its area since 1962, while the Lidder River watershed, which derives 60% of its annual runoff from snowmelt, has experienced significant declines in streamflow, particularly during peak summer months [15]. These changes are further compounded by extreme weather events such as hailstorms and floods, which disrupt livelihoods and ecosystems in the region [16]. This poses significant risks for smallholder farmers in Jammu and Kashmir, whose reliance on snow-fed irrigation leaves them vulnerable to water scarcity and unpredictable weather patterns [16]. These challenges highlight the urgency of developing adaptive strategies to enhance climate resilience, including improved forecasting systems, water-saving technologies, and sustainable agricultural practices [17].

This study aims to address these research gaps by analyzing snow accumulation (through SWE assessment) and snow cover trends in Jammu and Kashmir over the past 50 years. By examining the relationship between SWE, temperature, and wind speed, we try to assess the cascading impacts of snow resource variability on streamflow and water resource sustainability. The findings shall provide region-specific insights into the interconnected challenges of climate change, supporting the development of adaptive strategies for water resource management and climate resilience in this sensitive Himalayan region.

2. Materials and Methods

2.1. Study Area

The region of Jammu and Kashmir, located in northern India, lies between latitudes 32°17′ N to 36°58′ N and longitudes 73°26′ E to 80°30′ E [18]. This area exhibits significant geographical and climatic diversity, ranging from high-altitude, snow-covered mountains to fertile valleys [19]. The selected districts for this study consisted of Baramulla, Kupwara, Anantnag, Pulwama, Budgam, Shopian, Kulgam, Srinagar, Bandipora, and Ganderbal, which collectively represent the varied topographical and climatic conditions of the region. These districts were chosen due to their dependence on snowmelt for water resources and their vulnerability to the impacts of climate variability. The location of the study area is depicted in Figure 1.

The climate of Jammu and Kashmir is primarily influenced by its mountainous terrain, which governs its precipitation and temperature regimes. High-altitude districts such as Kupwara, Baramulla, and Bandipora experience significant snowfall during the winter, with temperatures often dropping below freezing. In contrast, mid- and low-elevation districts, including Srinagar and Pulwama, exhibit a temperate climate with moderate snowfall and relatively mild summers. To provide a comprehensive climatic characterization, long-term meteorological data from local weather stations were analyzed. The averages of annual precipitation, temperature, and snow depth were calculated, and their spatial distribution across districts was examined. These climatic parameters were further contextualized using the Thornthwaite climate classification system, enabling a systematic description of the region's climate variability.

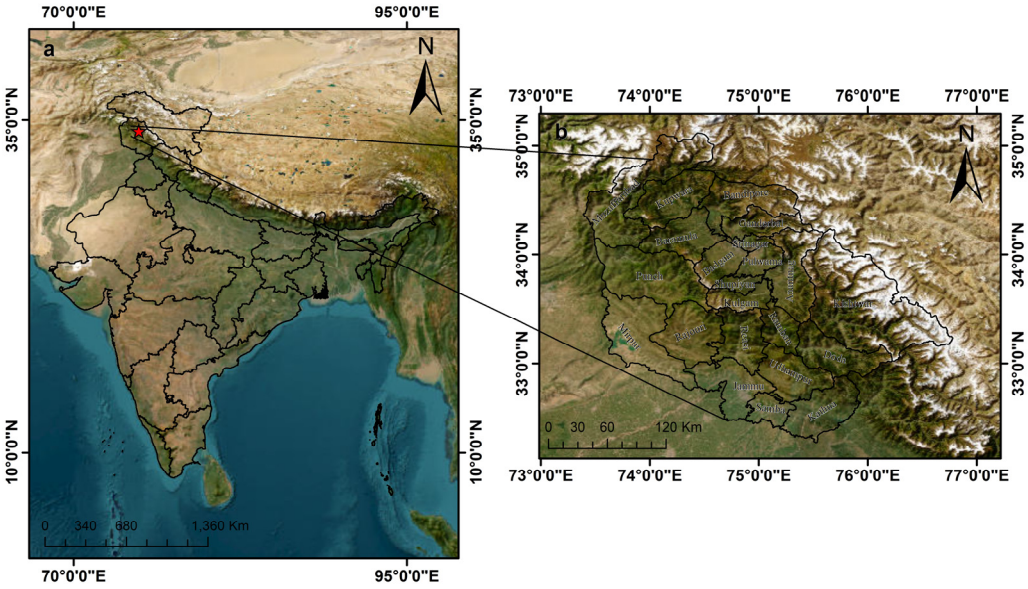

Figure 1. Location map of study area, (**a**) India, (**b**) Union Territory of Jammu and Kashmir.

2.2. Datasets

Multiple datasets were utilized to analyze the spatio-temporal variability in snow resources and associated climatic parameters from 1974 to 2024. ERA5 reanalysis data, sourced from the European Centre for Medium-Range Weather Forecasts (ECMWF), provided high-resolution information on temperature, wind speed, and SWE with a spatial resolution of 0.25° × 0.25° [20]. For validation purposes, ERA5 data were compared with IMD ground-based observations at weather stations located in Kupwara, Srinagar, and Qazigund. Three specific years, 1980, 1993, and 2014 were selected. For more recent years, the data were not available. Validation involved calculating Pearson's correlation coefficients as well as error metrics such as the root mean square error (RMSE) and mean absolute error (MAE).

Hydrological datasets, including runoff and streamflow volumes, were obtained from TerraClimate and processed using Google Earth Engine (GEE) [21]. These datasets were integrated to explore the interactions between snow resource variability, climatic parameters, and extreme weather events.

2.3. Methods

2.3.1. Snow Water Equivalent (SWE)

SWE is a critical metric for assessing water stored in snow and was calculated using Equation (1). It was used to examine the temporal trends in snow resources and their relationships with temperature and wind speed.

$$\text{SWE} = \text{Snow depth} \times (\text{Water density}/\text{Snow density}) \quad (1)$$

In this study, snow depth values were obtained from the ERA5 reanalysis dataset, which provides high-resolution snow-related parameters at a spatial resolution of 0.25° × 0.25° [22]. The density of water was assumed to be 1000 kg/m^3, while snow density values were derived from regional estimates and the literature, reflecting variations in snow compaction and seasonal conditions across the study area. The calculated SWE values enabled an assessment of the spatio-temporal variability in snow resources over the period 1974–2024. All the estimations were conducted in GEE.

2.3.2. Trend Analysis

To quantify the strength and direction of monotonic relationships between time-series variables, Kendall's Tau-b (K_j) was employed [23]. This non-parametric statistic extends the basic Kendall's Tau by incorporating adjustments for tied ranks, making it suitable for datasets where ties are prevalent. K_j was calculated using Equation (2)

$$K_j = \frac{S}{\sqrt{(n(n-1)\ 2-T_x)(\frac{n(n-1)}{2-T_y})}} \quad (2)$$

where S is the Mann–Kendall test statistic, calculated as the difference between the number of concordant (C) and discordant (D) pairs, $S = C - D$; n is the total number of observations. T_x and T_y are the number of tied ranks in the datasets being compared. This method provides a measure of correlation, ranging from −1 (perfect negative monotonic relationship) to 1 (perfect positive monotonic relationship), with 0 indicating no association. The normalization factor in the denominator adjusts for the number of possible pairs and tied ranks, ensuring the accuracy of K_j in datasets with varying distributions and ties. The statistical significance of K_j was assessed using a two-tailed hypothesis test. The null hypothesis (H_0) assumes no monotonic relationship between the variables, while the alternative hypothesis (H_1) suggests the existence of a monotonic relationship. p-values were derived at a 95% confidence level ($\alpha = 0.05$) to determine the statistical significance of the observed correlations.

Sen's Slope Estimator was used to quantify the magnitude of the identified trends. The slope ($Slope_k$) for all possible pairs of data points was calculated using Equation (3) [24]

$$Slope_k = \frac{x_j - x_i}{j - i} \quad (3)$$

The median of these slopes (β) represents the overall trend, as β = median ($Slope_k$), positive values of β indicate an upward trend, while negative values indicate a downward trend. Confidence intervals for β were computed at the 95% confidence level to assess the robustness of the results.

2.3.3. Zonal Statistics

To analyze spatial variability at the district level, zonal statistics were employed to calculate aggregated metrics from raster data [25]. This method was used to derive spatially aggregated values for SWE, temperature, and wind speed. The analysis utilized the

ArcGIS tool Zonal Statistics as Table, which integrates raster data with defined administrative boundaries.

2.3.4. Correlation Coefficient Calculation

The relationships between SWE, temperature, and wind speed were quantified using the Pearson correlation coefficient (r), a measure of the linear association between two variables [26]. The coefficient ranges from −1 to 1, where, $r = 1$ indicates a perfect positive correlation, $r = -1$ indicates a perfect negative correlation, and $r = 0$ indicates no correlation. This analysis was conducted at the district level to capture regional variations in these interactions. Significant correlations were further evaluated to understand the cascading effects of climatic changes on snow resources and related hydrological processes.

2.3.5. Spatio Temporal Distribution of Snow Cover Area

The spatio-temporal dynamics of snow cover were analyzed using Landsat satellite imagery for six selected years: 2000, 2005, 2010, 2015, 2020, and 2024. The Normalized Difference Snow Index (NDSI) [27] was utilized to detect snow-covered areas, calculated using the spectral bands of Landsat sensors as follows:

For Landsat 8 (LC08):

$$NDSI = \frac{(Band\ 3 - Band\ 6)}{(Band\ 3 + Band\ 6)} \quad (4)$$

where band 3 is the green band and band 6 is the SWIR band.

For Landsat 7 and Landsat 5:

$$NDSI = \frac{Band\ 2 - Band\ 5}{Band\ 2 + Band\ 5} \quad (5)$$

where band 2 is the green band and band 5 is the SWIR band.

The green band captures visible light reflectance, while the short-wave infrared (SWIR) band captures snow absorption properties. A threshold of 0.4 was applied to classify pixels as snow-covered. Temporal analyses were conducted using GEE to automate NDSI computations [28]. Spatial distribution patterns were further analyzed using GIS tools to classify snow cover and visualize its variation across the study area.

2.3.6. Annual Stream Flow Estimation

Annual streamflow for the study region was estimated using remote sensing data, hydrological modeling, and geospatial tools available within the GEE platform. Precipitation data from the NASA GPM IMERG dataset (2020) provided the input for estimating runoff [29], while land cover information from the COPERNICUS Land Cover dataset (2019) was used to assign land-use-specific runoff coefficients [30]. Flow accumulation data from the HydroSHEDS dataset were incorporated to identify areas of concentrated flow and to model hydrological pathways [31]. The calculation of streamflow (Q) was based on the following equation [32]

$$Q = R \times A \times \phi \quad (6)$$

where Q represents the streamflow volume in cubic meters per second (m^3), R is the runoff depth expressed in meters, A denotes the contributing drainage area in m^2, and ϕ serves as a hydrological scaling factor to ensure unit consistency. R was derived by multiplying the P by the runoff coefficient (C), which accounts for the proportion of precipitation that contributes to surface runoff. Runoff coefficients were assigned based on land cover types, with values ranging from 0.1 for permeable areas such as forests to 0.7 for impervious urban surfaces.

The precipitation data were spatially aggregated across the study region to calculate the annual total runoff. This process involved combining the derived runoff depth with the spatially distributed drainage area determined through flow accumulation analysis. Additionally, the ϕ was applied to convert units where necessary to ensure consistency between precipitation depth (e.g., mm/day) and streamflow volume (e.g., m^3). All data processing and hydrological modeling were conducted using GEE. The final streamflow volumes were computed at an annual scale and visualized to assess the temporal variability in water availability across the study region.

3. Results

3.1. Correlation of ERA5 Data with IMD

A comparison of mean monthly temperature data between ERA5 and IMD records for the years 1980, 1993, and 2014 was performed to evaluate the reliability of ERA5 as a dataset for regional climatological analyses in Jammu and Kashmir. Validation was conducted using ground-based observations from weather stations in Kupwara, Srinagar, and Qazigund. The results indicate a strong agreement between ERA5 and IMD datasets, as demonstrated by high Pearson correlation coefficients of 0.986 for 1980, 0.965 for 1993, and 0.977 for 2014. These findings confirm that ERA5 effectively captures the general temperature trends for the region. The RMSE values for 1980, 1993, and 2014 were 3.55, 3.87, and 3.26 °C, respectively, while the corresponding MAE values were 3.33, 3.22, and 2.90 °C. These relatively low error metrics suggest that ERA5 provides a reasonable representation of observed temperatures, with minor deviations evident in certain months. Specifically, variations are observed between the datasets for specific periods such as January and August, though the general alignment remains strong. Figure 2 illustrates the monthly temperature profiles for both datasets across the three analyzed years, and averaged for the three stations. While the overall patterns of seasonal temperature variation are consistent, ERA5 data occasionally deviate from IMD observations. These deviations appear more pronounced during certain months, though they do not significantly impact the strong agreement between the datasets. Such variations may reflect localized climatic influences that are not fully captured by the spatial resolution of ERA5. Additionally, due to observational data limitations, this validation was performed for only three years, and thus restricts a comprehensive assessment of ERA5 and IMD data over an extended time period. Incorporating longer time series data and conducting bias correction methods in future studies will enable a better evaluation and further refine the alignment between reanalysis and observational datasets.

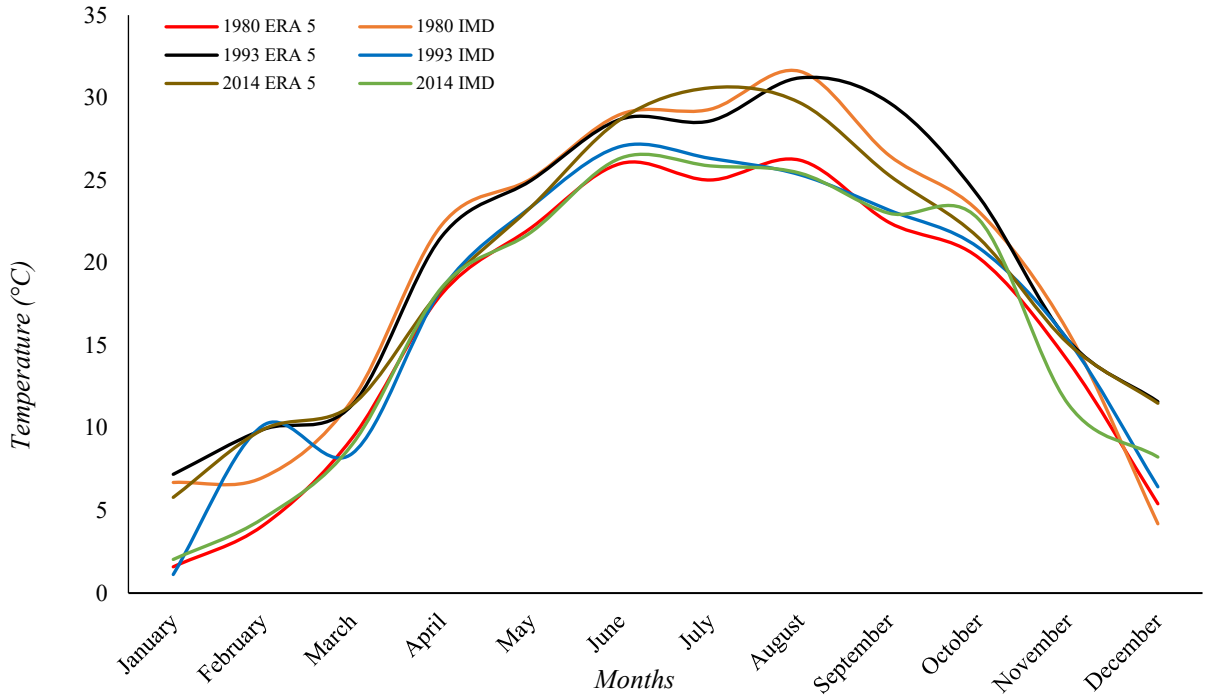

Figure 2. Comparison of monthly temperatures from ERA5 reanalysis data and IMD observations for 1980, 1993, and 2014.

3.2. Spatio Temporal Distribution of Snow Cover

The spatio-temporal analysis of snow cover across Jammu and Kashmir reveals a progressively deteriorating snow regime, with notable shifts in both the extent and intensity of snow-covered areas from 2000 to 2024. The snow-covered area experienced significant declines, with a steep reduction from 22,261.21 km² in 2000 to 15,275.75 km² in 2024. This marks a drastic 31.4% reduction over the study period, emphasizing the alarming rate at which snow resources are diminishing in this Himalayan region (Figures 3 and 4).

The NDSI maps (Figure 3a–f) illustrate these temporal changes, with high-altitude regions consistently maintaining higher NDSI values, which are generally indicative of snow presence. However, it is important to note that NDSI values are also influenced by surface reflectance characteristics, and factors such as older snow, meltwater over the snow, or impurities can lead to lower NDSI values, even in areas with dense snow cover. Despite this, high-altitude zones exhibit a gradual decline in snow presence over time, highlighting the impact of rising temperatures. In contrast, low-elevation areas in the southern regions show a steady retreat of snow-covered areas, with uncovered zones becoming increasingly pronounced by 2024. This highlights the heightened vulnerability of low-altitude regions to warming temperatures and shifting precipitation patterns. Anomalous rebounds in snow-covered areas, observed in 2015 and 2020, reflect short-term recoveries driven by localized weather events, such as increased winter precipitation in 2020. However, the rapid decline post-2020 highlights the transient nature of these anomalies in the face of long-term warming trends. The snow mask maps (Figure 4a–f) further illustrate these dynamics, showing that high-altitude northern regions remain critical snow reservoirs, with dense snowpacks persisting despite overall reductions. Transition zones between high and low NDSI areas, characterized by moderate snow cover, are expanding over time. The persistence of localized snow retention pockets, particularly in 2024, highlights the mitigating role of rugged topography and microclimatic conditions, such as shading and reduced wind exposure, in slowing snow loss. However, it must be acknowledged that the six NDSI maps, covering two decades, provide only snapshots of

snow cover dynamics and may not fully capture the year-to-year variability inherent in snow cover trends, and in future research, prioritization of high-resolution annual time series of NDSI data to better assess the inter-annual variability is required.

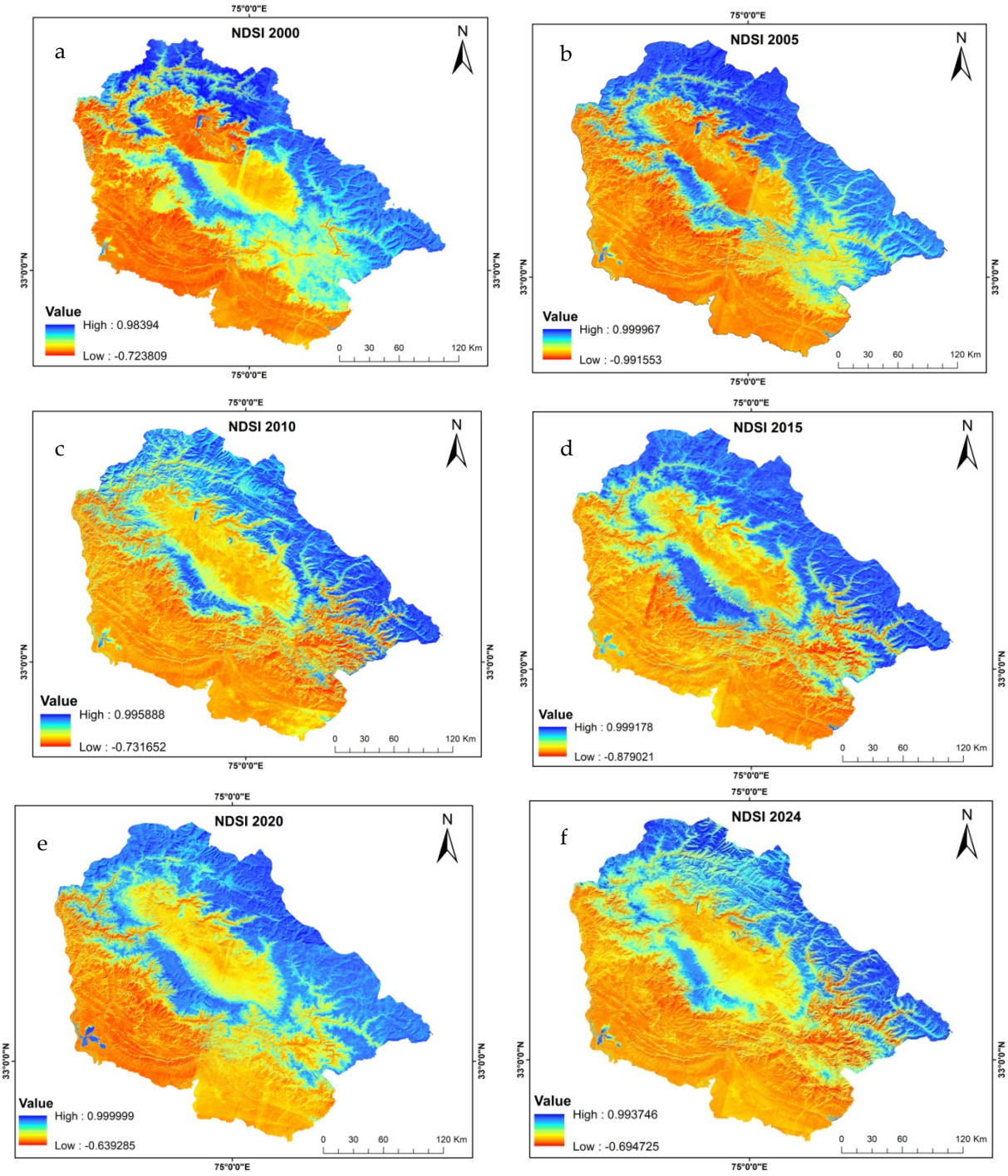

Figure 3. (**a**–**f**) These maps capture the evolving intensity and spatial dynamics of snow cover. The declining NDSI values post-2010 highlight the cumulative effects of rising temperatures, while the localized peaks in 2015 and 2020 hint at potential short-term climatic anomalies.

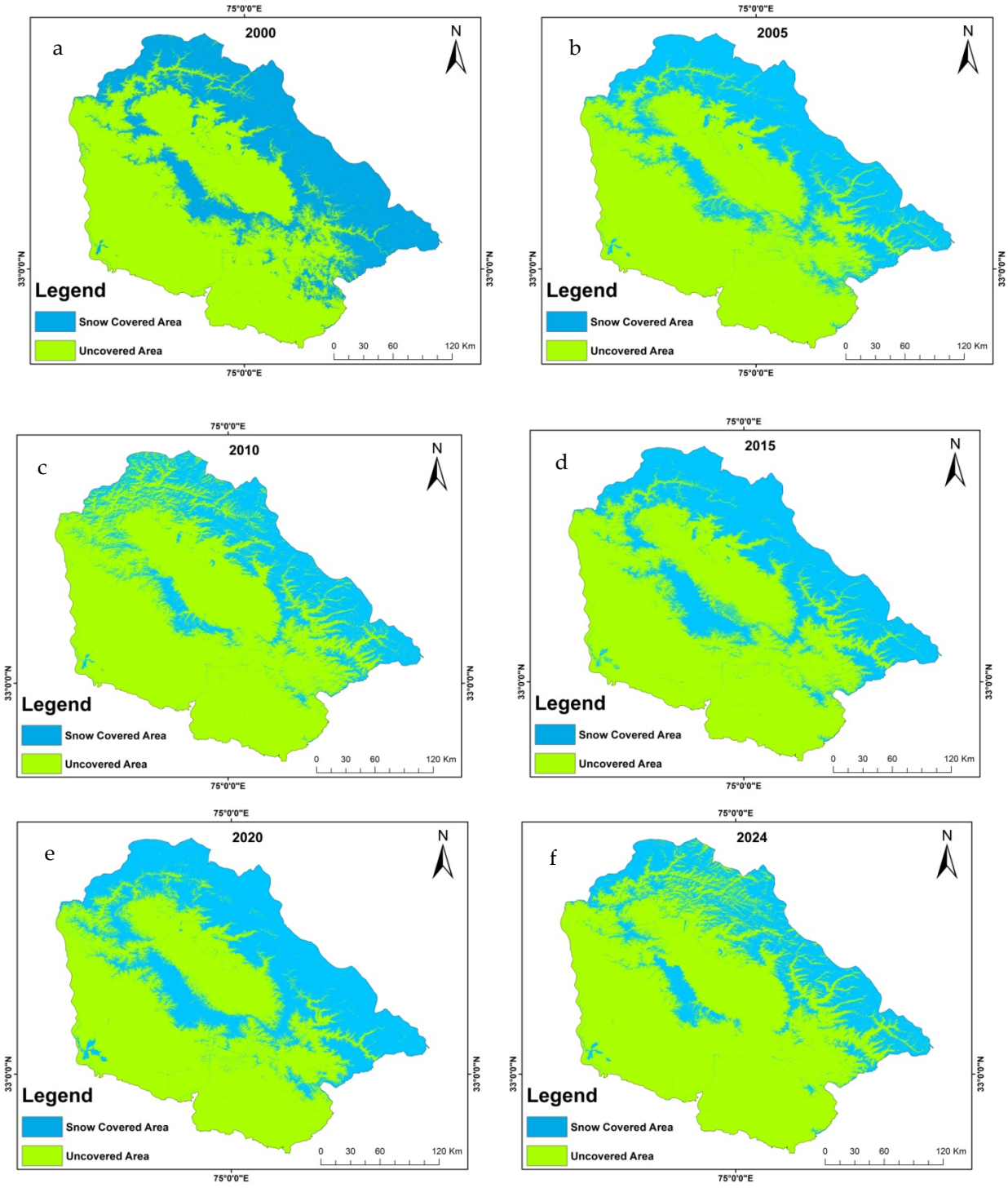

Figure 4. (**a**–**f**) The contrast between snow-covered and uncovered areas over time reveals the encroachment of barren zones into previously snow-dense regions. The persistence of high-altitude snowpacks amidst broader declines highlights their critical role as natural water reservoirs.

3.3. Streamflow Volume

The streamflow volumes for Jammu and Kashmir for the years 2000, 2005, 2010, 2015, 2020, and 2024 were derived from a geospatial hydrological model, integrating precipitation data, land cover-specific runoff coefficients, and flow accumulation datasets. The temporal evolution of streamflow volume is summarized in Table 1 and depicted in Figure 5, revealing a gradual increase over the 24-year study period, from 45.68 million m^3 in 2000 to 63.46 million m^3 in 2024—a substantial rise of approximately 38.8%.

Table 1. Estimated streamflow volume in years (2000–2024) in Jammu and Kashmir.

Year	Estimated Streamflow Volume (m^3)
2000	45,678,000
2005	52,345,000
2010	47,234,000
2015	55,890,000
2020	60,123,000
2024	63,456,000

The observed streamflow trends reflect the complex interplay between snowmelt, precipitation dynamics, and land use changes in the region (Figure 5). Early in the study period, the modest streamflow volumes recorded for 2000 and 2005 (45.68 million m^3 and 52.35 million m^3, respectively) align with relatively consistent snow cover levels observed in the NDSI maps for those years. These snowmelt contributions, combined with rainfall, suggest a more balanced hydrological regime during this period. However, the decline in streamflow volume to 47.23 million m^3 in 2010 is noteworthy and aligns with the marked reduction in snow-covered areas observed in the NDSI map for that year, where higher-elevation zones experienced significant snow depletion. This highlights the direct impact of snow cover loss on streamflow volume, as reduced snowmelt likely contributed to diminished surface runoff. While the NDSI snapshots provide avaluable insights into long-term snow cover trends, the absence of annual or monthly data as also discussed above, is one of the limitations of this study, which restricts our ability to quantify precise inter-annual changes in snow cover, to further strengthen the observed links between snow dynamics and hydrological responses.

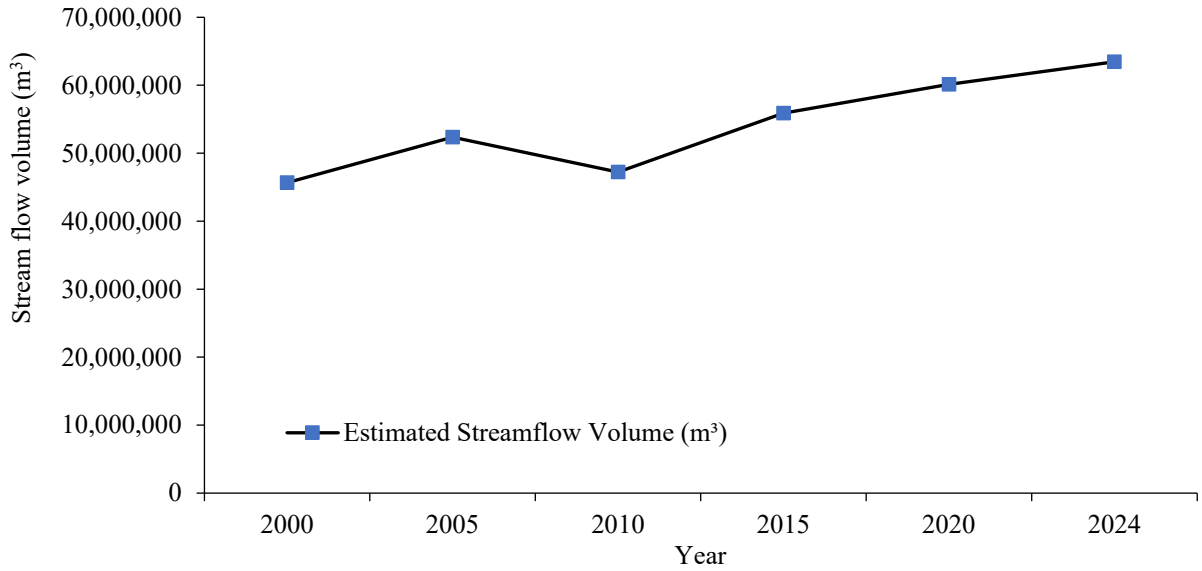

Figure 5. Temporal variation in estimated streamflow volumes (m^3) in Jammu and Kashmir for the years 2000, 2005, 2010, 2015, 2020, and 2024 derived using a geospatial hydrological model.

The subsequent years, particularly 2015 and 2020, show a resurgence in streamflow volumes, reaching 55.89 million m^3 and 60.12 million m^3, respectively. This increase corresponds to the temporary recovery of snow-covered areas evident in the NDSI maps, likely driven by localized climatic variations such as increased winter precipitation or colder temperatures during these years. The highest streamflow volume recorded in 2024 (63.46 million m^3) reflects the amplified contributions of rainfall and land cover transitions, as snow cover declines observed in the 2024 NDSI maps are offset by an increase in

precipitation intensity and surface runoff from urbanized areas. Urbanization and its associated impervious surfaces play a critical role in these streamflow dynamics. By reducing infiltration and accelerating runoff, urbanization amplifies streamflow volumes. This effect is particularly pronounced in lowland areas, where urban expansion has altered natural hydrological pathways. Our study's use of runoff coefficients of 0.7 for urban areas, 0.5 for forests, and 0.1 for other land types highlights the disproportionate contribution of urbanized regions to surface runoff and the transformative effects of land use changes on hydrological systems, as forests and permeable surfaces are replaced by impervious infrastructure. The integration of snow cover dynamics with streamflow estimates further reveals the cascading impacts of climate variability. The observed declines in snow cover post-2010 and particularly in 2024, as shown in the NDSI maps, underline the reduced snowmelt contributions to streamflow.

3.4. Trend Analysis of SWE

The analysis of SWE trends in the study area over the past 50 years reveals a consistent and statistically significant decline across most districts. Higher-elevation districts such as Kupwara and Bandipora exhibited the steepest reductions, with Sen's Slope values of −0.0003 and −0.0001 per year, respectively, indicating a gradual but meaningful downward trend (Figure 6, Table 2). While the yearly values may appear small, they represent significant cumulative changes over the study period, with long-term implications for snow resource availability and hydrological systems. These results, derived from the Mann–Kendall test and Sen's Slope estimator, highlight the critical vulnerability of snow resources in these regions to sustained climatic changes. Spatial patterns of SWE decline, as illustrated in Figure 6, reveal that higher-altitude areas are disproportionately affected, consistent with their greater dependency on seasonal snowmelt. The *p*-value map confirms that these trends are statistically significant, particularly in northern districts such as Kupwara and Bandipora, where climatic and topographic factors amplify the sensitivity of SWE to warming. By contrast, districts like Ganderbal and Pulwama show more moderate declines, reflecting localized variability in snow accumulation and melt dynamics.

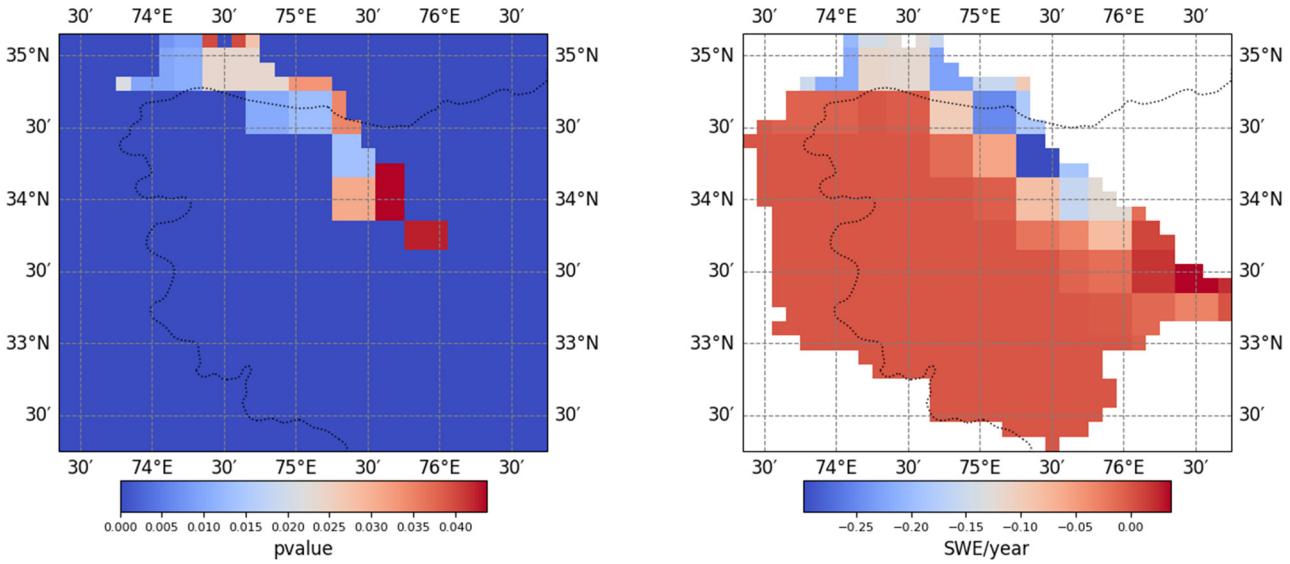

Figure 6. Spatial distribution of Sen's Slope estimates for SWE trends in Jammu and Kashmir from 1974 to 2024. The left inset illustrates the statistical significance (*p*-values) of the trends, while the right inset highlights the magnitude of SWE changes (SWE/year).

Declining SWE directly impacts the timing and magnitude of snowmelt, leading to reduced water availability during critical summer months. This aligns with the spatio-temporal snow cover analysis (Figures 3 and 4), which shows consistent reductions in snow-covered areas over the same period. The observed SWE declines correspond with trends in streamflow (Figure 5), suggesting that reduced snow storage capacity is contributing to altered hydrological cycles, particularly in watersheds like the Jhelum River Basin. These results hence highlight the urgent need to investigate the specific drivers of SWE decline, including rising temperatures and altered precipitation regimes, as observed in other sections of this study.

Table 2. Sen Slope of SWE in selected districts in Jammu and Kashmir.

District	Min	Max	Range	Mean	Std	Sum
Kupwara	−0.0003	0.0006	0.0009	0.0001	0.0002	0.0023
Bandipore	−0.0001	0.0016	0.0017	0.0003	0.0004	0.0080
Baramula	−0.0005	0.0003	0.0008	0.0000	0.0002	−0.0001
Ganderbal	0.0000	0.0016	0.0016	0.0002	0.0004	0.0032
Anantnag	−0.0001	0.0015	0.0016	0.0002	0.0004	0.0060
Srinagar	0.0001	0.0002	0.0002	0.0001	0.0001	0.0004
Badgam	0.0001	0.0005	0.0005	0.0002	0.0001	0.0027
Pulwama	−0.0001	0.0003	0.0004	0.0001	0.0001	0.0005
Shupiyan	0.0000	0.0002	0.0002	0.0001	0.0001	0.0007
Kulgam	0.0000	0.0003	0.0003	0.0001	0.0001	0.0012

3.5. Temperature Trends

The temperature trend analysis reveals a significant and widespread warming trend across all districts in Jammu and Kashmir over the past 50 years, as indicated by the Sen's Slope estimator and Mann–Kendall test results (Figure 7). The warming trend is consistent with global climate change patterns and is reflected in the mean temperature increases across the study area. The highest temperature increases were observed in Bandipora and Ganderbal, which exhibit notable Sen's Slope values of 0.00031 and 0.00024 °C/year, respectively (Table 3). In contrast, Srinagar and Pulwama show comparatively moderate warming, with Sen's Slope values of 0.00014 and 0.00006 °C/year, highlighting spatial variability in temperature changes.

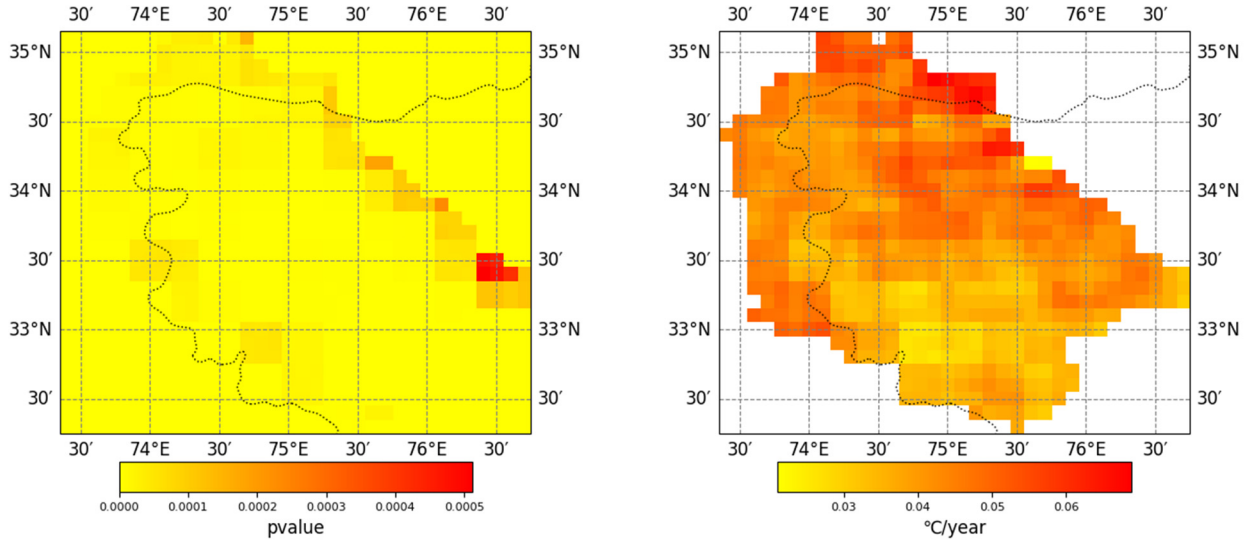

Figure 7. Spatial distribution of Sen's Slope estimates for mean temperature trends in Jammu and Kashmir from 1974 to 2024. The left inset depicts the statistical significance (*p*-values) of the observed trends, while the right inset shows the magnitude of temperature changes in °C per year.

The spatial distribution of warming trends shows increases in high-altitude districts such as Bandipora and Kupwara. These regions are particularly sensitive to climatic changes due to their topography and snow-dependent ecosystems. Conversely, districts like Baramulla show more modest changes, with fluctuations influenced by their diverse terrain and microclimatic conditions. The persistent warming, especially in winter months, contributes to reduced snowfall, earlier snowmelt, and subsequently, diminished snowpack, as evidenced by the concurrent decline in SWE and snow-covered areas (Figures 3, 4, and 6). Warmer winters exacerbate these changes, accelerating the hydrological shifts that impact water availability during critical summer months. This linkage between temperature increases and hydrological responses underscores the cascading effects of climate change on regional water resources. The *p*-value map (Figure 7, left inset) confirms the statistical significance of warming trends across most of the region, with the strongest signals observed in northern and central districts.

Table 3. Sen slope of mean temperature in selected districts in Jammu and Kashmir.

District	Min	Max	Range	Mean	Std	Sum
Kupwara	−0.00030	0.00050	0.00080	0.00010	0.00020	0.00200
Bandipora	−0.00010	0.00150	0.00160	0.00031	0.00037	0.00797
Baramulla	−0.00050	0.00028	0.00078	−0.00001	0.00022	−0.00011
Ganderbal	−0.00001	0.00157	0.00158	0.00024	0.00040	0.00316
Anantnag	−0.00013	0.00146	0.00159	0.00022	0.00038	0.00600
Srinagar	0.00007	0.00023	0.00016	0.00014	0.00007	0.00042
Badgam	0.00006	0.00051	0.00046	0.00023	0.00012	0.00272
Pulwama	−0.00008	0.00030	0.00037	0.00006	0.00011	0.00052
Shupiyan	0.00000	0.00023	0.00022	0.00010	0.00007	0.00069
Kulgam	0.00000	0.00034	0.00033	0.00012	0.00010	0.00123

3.6. Wind Speed

The analysis of wind speed trends in the study area over the past 50 years, as shown in Figure 8, highlights spatial variability in Sen's Slope values across districts. While certain areas, such as Kupwara and Bandipora, exhibited slight increases in wind speed, with notable Sen's Slope values around 0.0005, other districts, like Pulwama and Srinagar, showed near-neutral or marginally decreasing trends. This heterogeneity suggests localized climatic influences at play, likely shaped by topography, altitude, and microclimatic factors. Table 4 provides the statistical breakdown of wind speed trends, reflecting a mixed pattern across districts. For example, Kupwara's range of Sen's Slope values (−0.0003 to 0.00056) highlights significant variability, while Bandipora and Ganderbal consistently showed upward trends with mean values of 0.00031 and 0.00024, respectively. Conversely, districts such as Baramulla and Pulwama demonstrated relatively neutral or slightly negative trends, indicating minimal or no changes over time.

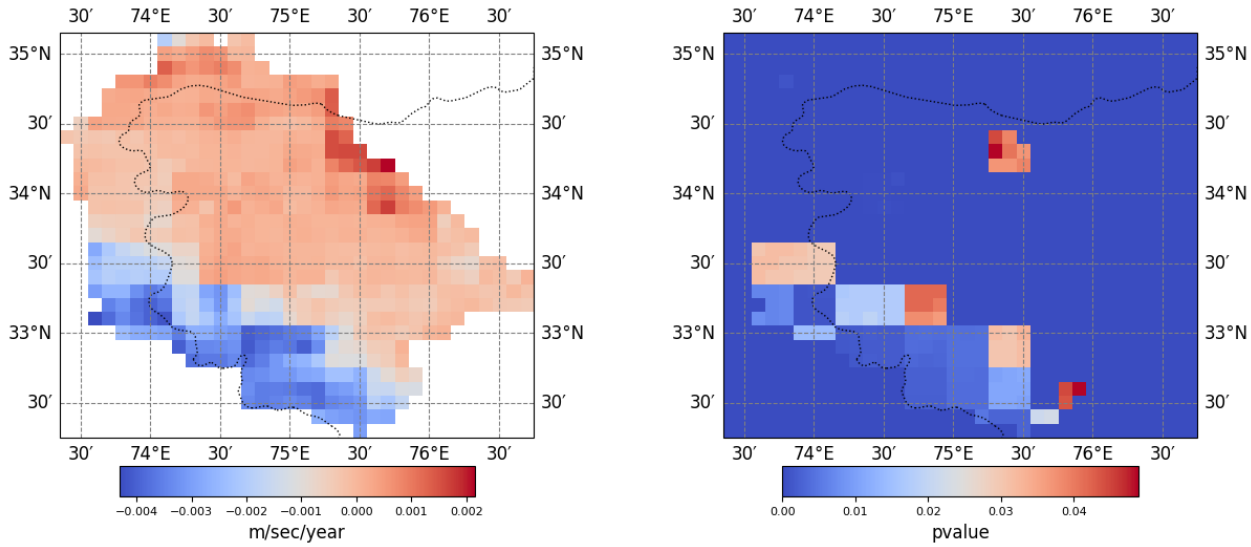

Figure 8. Sen's Slope estimates for wind speed trends (**left**) and their corresponding *p*-values (**right**) across Jammu and Kashmir over the past 50 years.

From a spatial understanding, the southern regions of Jammu and Kashmir exhibited near-stagnant or decreasing wind speeds, as depicted by cooler tones in Figure 8 (left inset). In contrast, the northern high-altitude districts experienced subtle increases in wind speed, marked by warmer tones in the same figure. However, the statistical significance of these trends remains inconsistent, with fewer districts demonstrating *p*-values below 0.05 (Figure 8, right inset), indicating limited reliability of the observed trends across the entire region.

Table 4. Sen slope estimate of wind speed in selected districts in Jammu and Kashmir.

District	Min	Max	Range	Mean	Std	Sum
Kupwara	−0.00030	0.00056	0.00086	0.00010	0.00021	0.00231
Bandipore	−0.00013	0.00156	0.00169	0.00031	0.00037	0.00797
Baramula	−0.00050	0.00028	0.00078	−0.00001	0.00022	−0.00011
Ganderbal	−0.00001	0.00157	0.00158	0.00024	0.00040	0.00316
Anantnag	−0.00013	0.00146	0.00159	0.00022	0.00038	0.00600
Srinagar	0.00007	0.00023	0.00016	0.00014	0.00007	0.00041
Badgam	0.00006	0.00051	0.00046	0.00023	0.00012	0.00272
Pulwama	−0.00007	0.00030	0.00037	0.00006	0.00011	0.00052
Shupiyan	0.00000	0.00023	0.00022	0.00010	0.00007	0.00069
Kulgam	0.00000	0.00034	0.00033	0.00012	0.00010	0.00123

3.7. Correlation Analysis

The correlation analysis between SWE, mean temperature, and wind speed across the study area provides critical insights into the interrelationships of these climatic variables (Figure 9). A significant negative correlation was observed between SWE and mean temperature, with correlation coefficients ranging from −0.7 to −0.9. The statistical significance of these correlations was assessed using a t-test for Pearson correlation coefficients, with the null hypothesis (H0) assuming no correlation between the variables. The p-values derived from this test confirmed that these relationships are statistically significant at the 95% confidence level ($p < 0.05$), showing that as temperatures rise, snowpack levels decrease. The implications of this finding are clear, as warmer temperatures reduce snow accumulation as well as lead to earlier snowmelt, thereby influencing water availability during critical periods. This pattern aligns with global trends, where rising temperatures

are consistently linked to declining SWE [33]. In contrast, the relationship between SWE and wind speed was weaker, with correlation coefficients ranging from −0.2 to −0.4. Although a slight negative trend was observed, the weak correlation indicates that wind speed plays a less significant role in influencing SWE on a broader scale. Localized effects of wind, such as snow redistribution and increased evaporation, may occur, but they do not appear to substantially contribute to the overall reduction in SWE across the region.

The correlation between mean temperature and wind speed was found to be mildly positive, with coefficients ranging from 0.3 to 0.5. This suggests that warmer temperatures may be modestly associated with higher wind speeds, potentially due to increased atmospheric instability during warmer months [34]. While this relationship may indirectly influence snowmelt by increasing evaporation rates, its impact is secondary to the more direct influence of temperature on SWE. Significance testing, with a *p*-value threshold of 0.05, confirmed that the strongest and most consistent relationships were observed between SWE and temperature. This finding reinforces the pivotal role of temperature as a driver of snowpack dynamics [35]. The weak correlations between wind speed and SWE, as well as between wind speed and temperature, highlight the secondary and localized effects of wind in shaping SWE trends [36].

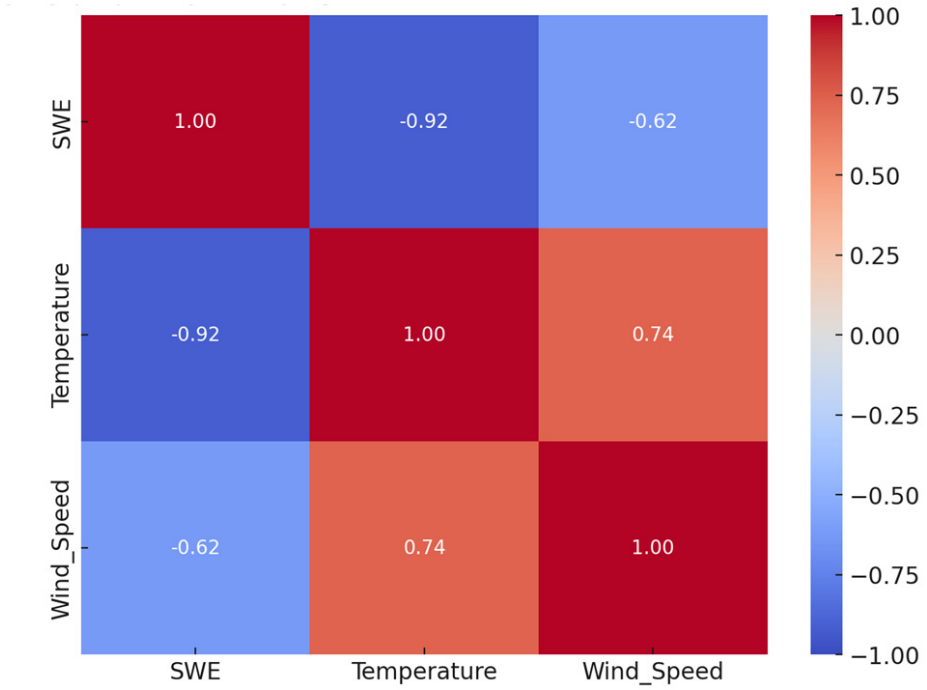

Figure 9. Heat map showing the correlation coefficients between SWE, temperature, and wind speed, across the study area.

4. Discussion

This study demonstrates a strong correlation between IMD and ERA5 datasets for temperature in Jammu and Kashmir, reaffirming the reliability of ERA5 for regional climate analyses. The observed agreement aligns with previous studies validating ERA5 for meteorological assessments across India, particularly during extreme heatwave events in urban areas [37,38]. Similarly, studies comparing ERA5 reanalysis with ground-based GNSS-derived Integrated Precipitable Water Vapor (IPWV) have reported high accuracy (correlation coefficients exceeding 0.97), further validating the robustness of ERA5 in mountainous terrains [39]. Our results reveal a significant and widespread decline in SWE across Jammu and Kashmir over the past five decades, consistent with global patterns in diminishing snowpacks [40]. The steepest declines were observed in high-altitude

districts like Kupwara and Bandipora, where Sen's Slope values (−0.0003 and −0.0001, respectively) highlight their vulnerability to warming trends. These findings align with studies in the Hindu Kush–Himalayan region that report significant snow depth and SWE reductions, particularly in areas affected by rapid glacier retreat [41–43]. The phenomenon of "warm snow drought", where warmer winters reduce snow accumulation despite stable precipitation, is evident in our study [44]. This aligns with global observations that rising temperatures cause precipitation to fall as rain instead of snow, coupled with earlier snowmelt [45].

The integration of SWE, temperature, and wind speed data provides insights into the dynamics of snowpack changes. The strong negative correlation between SWE and temperature ($r = -0.92$) highlights temperature as the primary driver of snow loss, while wind speed shows a weaker influence on SWE, likely limited to localized effects such as redistribution and sublimation [46]. Studies suggest that wind primarily impacts snow under specific conditions [47], and its role is secondary compared to temperature-induced changes [48]. The cascading impacts of SWE decline on water resources are evident in our analysis. Reduced SWE translates into diminished snowmelt contributions to summer streamflows [49], as evidenced by declining trends in high-altitude districts like Kupwara and Bandipora. This has significant implications for agriculture, hydropower, and water availability during critical growing seasons [50]. Adaptive water management strategies, including advanced snow monitoring systems, efficient irrigation techniques, and real-time dam inflow monitoring, are necessary to mitigate these impacts [51]. For example, regions like Kupwara, which exhibit steep SWE declines, face increased challenges in sustaining water supplies for agriculture and hydropower during dry periods. Furthermore, an intriguing aspect of this study is the relationship between SWE decline and hailstorm events. Hailstorm frequency data from 2007–2022 reveal variations across districts, with high-altitude regions like Baramulla and Kupwara reporting 37 and 29 hailstorm events, respectively, during this period [16]. These districts, characterized by sharp SWE declines and significant temperature increases, may be experiencing heightened atmospheric instability conducive to hailstorm formation [52]. While temperature rise appears to be a dominant factor, reduced snow cover may also contribute by altering surface albedo and increasing atmospheric instability [53]. In contrast, lower-elevation districts like Ganderbal, which experienced only 10 hailstorm events, align with their more moderate SWE decline and temperature trends. These findings suggest a potential link between SWE reduction and hailstorm frequency, although additional studies are required to confirm this interaction.

The socioeconomic implications of these climatic changes are significant, particularly for smallholder farmers reliant on snowmelt for irrigation [54]. The unpredictable water availability, coupled with extreme weather events like hailstorms, threatens agricultural productivity and livelihood security [55]. For instance, Baramulla and Kupwara, which reported higher hailstorm frequencies, are also districts where farmers have reported significant crop damage due to these events. Adaptive measures such as crop diversification, weather-indexed insurance, and sustainable agricultural practices could mitigate the risks posed by climate change on livelihoods in Jammu and Kashmir [56]. Initiatives like the Jammu and Kashmir Rural Livelihoods Mission demonstrate the potential of integrating community-based approaches with technological advancements to enhance resilience [54,57]. The observed interplay between SWE decline, rising temperatures, and hailstorm frequency highlights the need for region-specific strategies to mitigate the impacts of climate change on snow resources and extreme weather events.

5. Conclusions

This study presents an analysis of climatic trends and their hydrological implications for Jammu and Kashmir, focusing on SWE, temperature, snow cover, wind speed, and streamflow dynamics. Using multi-source datasets and advanced analytical methods, climatic trends over the past five decades were observed. Notable findings include a measurable decline in SWE, particularly in high-altitude districts such as Kupwara and Bandipora, as shown by Sen's Slope analysis and Mann–Kendall test results. These trends are linked to rising temperatures and altered precipitation patterns, which contribute to earlier snowmelt and reduced snow cover duration. The spatio-temporal distribution of snow cover, analyzed through NDSI, highlights regional vulnerability to climate variability, with implications for water resources and ecosystems. Despite these findings, the study acknowledges various limitations. The spatial resolution of datasets like ERA5 reanalysis limits the ability to capture fine-scale climate variations in complex mountainous terrain. Additionally, generalized runoff coefficients used in streamflow modeling may not fully account for localized hydrological processes, and the model does not explicitly incorporate snowmelt dynamics, which are critical contributors to annual streamflows in the Kashmir Valley. Moreover, the generalized hydrological parameters used may not fully reflect the distinct climatic and topographical differences between districts in the Kashmir Valley and the Jammu region, potentially affecting the model's accuracy. The pearson correlation employed to validate ERA5 temperature data, although demonstrated strong alignment with IMD data, may not fully capture subtle but critical deviations that significantly would influence snowmelt and SWE dynamics. Therefore, alternative metrics like Percent Bias (PBias) will provide a better evaluation of dataset reliability and its implications for snow hydrology studies in the region. Further the secondary hailstorm data lacked detailed meteorological variables necessary for better analysis. Therefore, future research must incorporate higher-resolution datasets, localized hydrological parameters, and long-term monitoring of SWE through remote sensing and ground-based systems to refine predictive capabilities and inform policy development.

Author Contributions: Conceptualization, S.K., A.A.B., and S.K.S.; Methodology, S.K., S.K.S., S.K.G., P.K., and A.A.B.; Software, P.D.D., S.K.G., B.S., and A.A.B.; Validation, S.K., P.K., A.A.B., and S.K.G.; Formal Analysis, S.K., A.A.B., P.K., and S.K.G.; Investigation, S.K., and S.K.G.; Resources, S.K. and P.K.; Data Curation, S.K. and P.K.; Writing—Original Draft Preparation, S.K., A.A.B., P.D.D. and S.K.G.; Writing—Review and Editing, S.K.S., and G.M.; Visualization, B.S., and S.K.S.; Supervision, S.K. and S.K.S.; Project Administration, S.K.S. All authors have read and agreed to the published version of the manuscript.

Funding: This research received no external funding.

Data Availability Statement: The data are available from the first author on request.

Acknowledgments: We extend our gratitude to the United States Geological Survey (USGS) for supplying the indispensable Landsat data, and to Google Earth Engine for the provision of their robust analytical platform, which significantly facilitated our research. Furthermore, we sincerely appreciate the valuable insights and constructive feedback provided by four anonymous reviewers, whose diligent work and thoughtful suggestions have significantly enriched the quality and depth of this manuscript.

Conflicts of Interest: The authors declare no conflicts of interest.

References

1. Yang, D.; Yang, Y.; Xia, J. Hydrological cycle and water resources in a changing world: A review. *Geogr. Sustain.* **2021**, *2*, 115–122.
2. Siirila-Woodburn, E.R.; Rhoades, A.M.; Hatchett, B.J.; Huning, L.S.; Szinai, J.; Tague, C.; Nico, P.S.; Feldman, D.R.; Jones, A.D.; Collins, W.D.; et al. A low-to-no snow future and its impacts on water resources in the western United States. *Nat. Rev. Earth Environ.* **2021**, *2*, 800–819.
3. Viviroli, D.; Archer, D.R.; Buytaert, W.; Fowler, H.J.; Greenwood, G.B.; Hamlet, A.F.; Huang, Y.; Koboltschnig, G.; Litaor, M.I.; López-Moreno, J.I.; et al. Climate change and mountain water resources: Overview and recommendations for research, management and policy. *Hydrol. Earth Syst. Sci.* **2011**, *15*, 471–504.
4. Ding, Y.; Zhang, S.; Chen, R. Cryospheric hydrology: Decode the largest freshwater reservoir on earth. *Bull. Chin. Acad. Sci. (Chin. Version)* **2020**, *35*, 414–424.
5. Weiskopf, S.R.; Rubenstein, M.A.; Crozier, L.G.; Gaichas, S.; Griffis, R.; Halofsky, J.E.; Hyde, K.J.; Morelli, T.L.; Morisette, J.T.; Muñoz, R.C.; et al. Climate change effects on biodiversity, ecosystems, ecosystem services, and natural resource management in the United States. *Sci. Total Environ.* **2020**, *733*, 137782.
6. Kumar, A.; Sharma, N.; Ahmad, M.; Siddiqui, M.W. Climate change, food security, and livelihood opportunities in mountain agriculture. *Clim. Dyn. Hortic. Sci.* **2015**, *28*, 349–360.
7. Barry, R.G. Mountain climatology and past and potential future climatic changes in mountain regions: A review. *Mt. Res. Dev.* **1992**, *12*, 71–86.
8. Pomeroy, J.W.; Brun, E. Physical properties of snow. *Snow Ecol. Interdiscip. Exam. Snow-Cover. Ecosyst.* **2001**, *45*, 118.
9. Nastos, P.T.; Dalezios, N.R. Preface: Advances in meteorological hazards and extreme events. *Nat. Hazards Earth Syst. Sci.* **2016**, *16*, 1259–1268.
10. Brandt, W.T. *A Solution to One of Mountain Hydrology's Principal Mysteries: The Spatial Distribution of Snowfall*; University of California, Santa Barbara: Santa Barbara, CA, USA, 2019.
11. Franz, K.J.; Hogue, T.S.; Barik, M.; He, M. Assessment of SWE data assimilation for ensemble streamflow predictions. *J. Hydrol.* **2014**, *519*, 2737–2746.
12. Yadav, J.S.; Tiwari, S.K.; Misra, A.; Rai, S.K.; Yadav, R.K. High-altitude meteorology of Indian Himalayan Region: Complexities, effects, and resolutions. *Environ. Monit. Assess.* **2021**, *193*, 1–29.
13. Huda, M.B.; Kumar, R.; Rather, N.A. Water Resources Scenario of Indian Himalayan Region. In *Applied Agricultural Practices for Mitigating Climate Change*; CRC Press: Boca Raton, FL, USA, 2019; Volume 2, pp. 257–274.
14. Shafiq, M.U.; Rasool, R.; Ahmed, P.; Dimri, A.P. Temperature and precipitation trends in Kashmir Valley, Northwestern Himalayas. *Theor. Appl. Climatol.* **2019**, *135*, 293–304.
15. Ahmed, R.; Rawat, M.; Wani, G.F.; Ahmad, S.T.; Ahmed, P.; Jain, S.K.; Meraj, G.; Mir, R.A.; Rather, A.F.; Farooq, M. Glacial lake outburst flood hazard and risk assessment of Gangabal Lake in the Upper Jhelum Basin of Kashmir Himalaya using geospatial technology and hydrodynamic modeling. *Remote Sens.* **2022**, *14*, 5957.
16. Bhat, M.S.; Mir, S.; Parrey, H.A.; Thoker, I.A.; Shah, S.A. Climate change, hailstorm incidence, and livelihood security: A perspective from Kashmir valley India. *Nat. Hazards* **2024**, *120*, 2803–2827.
17. Garwi, J.; Masengu, R.; Chiwaridzo, O.T. (Eds.) *Emerging Technologies and Marketing Strategies for Sustainable Agriculture*; IGI Global: Hershey, PA, USA, 2024.
18. Taufique, M.; Khursheed, V. Status of horticulture in Jammu and Kashmir: An overview. *Geographer* **2018**, *65*, 78–87.
19. Sharma, N.; Raina, A.K. Composition, structure and diversity of tree species along an elevational gradient in Jammu province of north-western Himalayas, Jammu and Kashmir, India. *J. Biodivers. Environ. Sci.* **2013**, *3*, 12–23.
20. Muñoz-Sabater, J.; Dutra, E.; Agustí-Panareda, A.; Albergel, C.; Arduini, G.; Balsamo, G.; Boussetta, S.; Choulga, M.; Harrigan, S.; Hersbach, H.; et al. ERA5-Land: A state-of-the-art global reanalysis dataset for land applications. *Earth Syst. Sci. Data* **2021**, *13*, 4349–4383.
21. Singh, V.K.; Pandey, H.K.; Singh, S.K. Groundwater storage change estimation using GRACE data and Google Earth Engine: A basin scale study. *Phys. Chem. Earth Parts A/B/C* **2023**, *129*, 103297.
22. Zhang, H.; Zhang, F.; Che, T.; Yan, W.; Ye, M. Investigating the ability of multiple reanalysis datasets to simulate snow depth variability over mainland China from 1981 to 2018. *J. Clim.* **2021**, *34*, 9957–9972.
23. Parker, R.I.; Vannest, K.J.; Davis, J.L.; Sauber, S.B. Combining nonoverlap and trend for single-case research: Tau-U. *Behav. Ther.* **2011**, *42*, 284–299.

24. Nita, M.; Ellis, M.A.; Madden, L.V. Reliability and accuracy of visual estimation of Phomopsis leaf blight of strawberry. *Phytopathology* **2003**, *93*, 995–1005.
25. Singla, S.; Eldawy, A. Raptor zonal statistics: Fully distributed zonal statistics of big raster+ vector data. In Proceedings of the 2020 IEEE International Conference on Big Data (Big Data), Atlanta, GA, USA, 10–13 December 2020; IEEE: Piscataway, NJ, USA, 2020; pp. 571–580.
26. Tong, S.; Wong, N.H.; Jusuf, S.K.; Tan, C.L.; Wong, H.F.; Ignatius, M.; Tan, E. Study on correlation between air temperature and urban morphology parameters in built environment in northern China. *Build. Environ.* **2018**, *127*, 239–249.
27. Hall, D.K.; Riggs, G.A. Normalized-difference snow index (NDSI). In *Encyclopedia of Snow, Ice and Glaciers*; Singh, V.P., Singh, P., Haritashya, U.K., Eds.; Springer: Dordrecht, The Netherlands, 2011; pp. 779–780. ISBN 978-90-481-2642-2.
28. Su, Y.; Wu, S.; Kang, S.; Xu, H.; Liu, G.; Qiao, Z.; Liu, L. Monitoring Cropland Abandonment in Southern China from 1992 to 2020 Based on the Combination of Phenological and Time-Series Algorithm Using Landsat Imagery and Google Earth Engine. *Remote Sens.* **2023**, *15*, 669.
29. Pradhan, R.K.; Markonis, Y.; Godoy, M.R.V.; Villalba-Pradas, A.; Andreadis, K.M.; Nikolopoulos, E.I.; Papalexiou, S.M.; Rahim, A.; Tapiador, F.J.; Hanel, M. Review of GPM IMERG performance: A global perspective. *Remote Sens. Environ.* **2022**, *268*, 112754.
30. Bhattacharjee, J.; Marttila, H.; Launiainen, S.; Lepistö, A.; Kløve, B. Combined use of satellite image analysis, land-use statistics, and land-use-specific export coefficients to predict nutrients in drained peatland catchment. *Sci. Total Environ.* **2021**, *779*, 146419.
31. Xie, H.; Longuevergne, L.; Ringler, C.; Scanlon, B.R. Calibration and evaluation of a semi-distributed watershed model of Sub-Saharan Africa using GRACE data. *Hydrol. Earth Syst. Sci.* **2012**, *16*, 3083–3099.
32. Huang, S.; Chang, J.; Huang, Q.; Chen, Y. Monthly streamflow prediction using modified EMD-based support vector machine. *J. Hydrol.* **2014**, *511*, 764–775.
33. Smith, T.; Bookhagen, B. Changes in seasonal snow water equivalent distribution in High Mountain Asia (1987 to 2009). *Sci. Adv.* **2018**, *4*, e1701550.
34. Salinger, M.J. Climate variability and change: Past, present and future—An overview. *Clim. Change* **2005**, *70*, 9–29.
35. Hamlet, A.F.; Mote, P.W.; Clark, M.P.; Lettenmaier, D.P. Effects of temperature and precipitation variability on snowpack trends in the western United States. *J. Clim.* **2005**, *18*, 4545–4561.
36. Winstral, A.; Marks, D.; Gurney, R. Simulating wind-affected snow accumulations at catchment to basin scales. *Adv. Water Resour.* **2013**, *55*, 64–79.
37. Gupta, P.; Verma, S.; Mukhopadhyay, P.; Bhatla, R.; Payra, S. Fidelity of WRF model in simulating heat wave events over India. *Sci. Rep.* **2024**, *14*, 2693.
38. Mishra, Y.K.; Singh, A.; Patel, P.K. Investigation of the Indian Summer and Correlation between IMD and ERA5 Dataset. *World J. Adv. Res. Rev.* **2023**, *19*, 1187–1197.
39. Tomar, C.S.; Bhatla, R.; Singh, N.L.; Soni, V.K. Inter-Comparison of GNSS-IPWV with ERA-5 IPWV over the Indian Region. *MAUSAM* **2024**, *75*, 1085–1094.
40. Mote, P.W.; Li, S.; Lettenmaier, D.P.; Xiao, M.; Engel, R. Dramatic declines in snowpack in the western US. *Npj Clim. Atmos. Sci.* **2018**, *1*, 2.
41. Terzago, S.; von Hardenberg, J.; Palazzi, E.; Provenzale, A. Snowpack Changes in the Hindu Kush–Karakoram–Himalaya from CMIP5 Global Climate Models. *J. Hydrometeorol.* **2014**, *15*, 2293–2313. https://doi.org/10.1175/JHM-D-13-0196.1.
42. Notarnicola, C. Observing Snow Cover and Water Resource Changes in the High Mountain Asia Region in Comparison with Global Mountain Trends over 2000–2018. *Remote Sens.* **2020**, *12*, 3913. https://doi.org/10.3390/rs12233913
43. Smith, T., Bookhagen, B. and Rheinwalt, A. Spatiotemporal patterns of High Mountain Asia's snowmelt season identified with an automated snowmelt detection algorithm, 1987–2016. *Cryosphere* **2017,** *11*, 2329-2343. https://doi.org/10.5194/tc-11-2329-2017.
44. Harpold, A.A.; Dettinger, M.; Rajagopal, S. Defining snow drought and why it matters. *Eos* **2017**, *98*. https://doi.org/10.1029/2017EO068775.
45. Adam, J.C.; Hamlet, A.F.; Lettenmaier, D.P. Implications of global climate change for snowmelt hydrology in the twenty-first century. *Hydrol. Process. Int. J.* **2009**, *23*, 962–972.
46. Winkler, R.D.; Moore, R.D.; Redding, T.E.; Spittlehouse, D.L.; Carlyle-Moses, D.E.; Smerdon, B.D. Hydrologic processes and watershed. In *Compendium of Forest Hydrology and Geomorphology in British Columbia*; Ministry of Forests and Range: Victoria, BC, Canada, 2010; Volume 66, p. 133.
47. Mott, R.; Vionnet, V.; Grünewald, T. The seasonal snow cover dynamics: Review on wind-driven coupling processes. *Front. Earth Sci.* **2018**, *6*, 197.

48. Templer, P.H.; Reinmann, A.B.; Sanders-DeMott, R.; Sorensen, P.O.; Juice, S.M.; Bowles, F.; Sofen, L.E.; Harrison, J.L.; Halm, I.; Rustad, L.; et al. Climate Change Across Seasons Experiment (CCASE): A new method for simulating future climate in seasonally snow-covered ecosystems. *PLoS ONE* **2017**, *12*, e0171928.
49. Aili, T.; Soncini, A.; Bianchi, A.; Diolaiuti, G.; D'Agata, C.; Bocchiola, D. Assessing water resources under climate change in high-altitude catchments: A methodology and an application in the Italian Alps. *Theor. Appl. Climatol.* **2019**, *135*, 135–156.
50. Momblanch, A.; Holman, I.P.; Jain, S.K. Current Practice and Recommendations for Modelling Global Change Impacts on Water Resource in the Himalayas. *Water* **2019**, *11*, 1303. https://doi.org/10.3390/w11061303
51. Holland, M. Development and Validation of Monitoring Technologies to Support Water Resource Policy Compliance in the Western United States. Doctoral Dissertation, University of Colorado at Boulder, Boulder, CO, USA, 2023.
52. Trefalt, S.; Martynov, A.; Barras, H.; Besic, N.; Hering, A.M.; Lenggenhager, S.; Noti, P.; Röthlisberger, M.; Schemm, S.; Germann, U.; et al. A severe hail storm in complex topography in Switzerland-Observations and processes. *Atmos. Res.* **2018**, *209*, 76–94.
53. Yi, Y.; Kimball, J.S.; Rawlins, M.A.; Moghaddam, M.; Euskirchen, E.S. The role of snow cover affecting boreal-arctic soil freeze–thaw and carbon dynamics. *Biogeosciences* **2015**, *12*, 5811–5829.
54. Hussain, A.; Qamar, F.M.; Adhikari, L.; Hunzai, A.I.; Rehman, A.u.; Bano, K. Climate Change, Mountain Food Systems, and Emerging Opportunities: A Study from the Hindu Kush Karakoram Pamir Landscape, Pakistan. *Sustainability* **2021**, *13*, 3057. https://doi.org/10.3390/su13063057
55. Narayan, M.; Singh, N.; Solanki, P.; Srivastava, R.K. Impact of Extreme Events on Global Food Security. In *Food Security in a Developing World: Status, Challenges, and Opportunities*; Springer Nature: Cham, Switzerland, 2024; pp. 133–152.
56. Kaur, K.; Kaur, J.; Singh, R. Climate Resilient Agriculture: Binding Agriculture Innovations and Insurance. In *The Impact of Climate Change and Sustainability Standards on the Insurance Market*; Scrivener Publishing: Beverly, MA, USA, 2023; pp. 107–126.
57. Katoch, O.R.; Ahemad, S. Role of Self-help Groups (SHGs) in Enhancing Incomes of Rural Women in J&K, India. *South Asian J. Soc. Stud. Econ.* **2022**, *16*, 24–32.